The Pharmacokinetics of Individual Conjugated Xanthohumol Metabolites Show Efficient Glucuronidation and Higher Bioavailability of Micellar than Native Xanthohumol in a Randomized, Double-Blind, Crossover Trial in Healthy Humans

Lance Buckett, Nadine Sus, Veronika Spindler, Michael Rychlik, Christian Schoergenhofer,* and Jan Frank*

Scope: Prenylated chalcones and flavonoids are found in many plants and are believed to have beneficial effects on health when consumed. Xanthohumol is present in beer and likely the most consumed prenylated chalcone, but poorly absorbed and rapidly metabolized and excreted, thus limiting its bioavailability. Micellar formulations of phytochemicals have been shown to improve bioavailability.

Methods and results: In a randomized, double-blind, crossover trial with five healthy (three males and two females) volunteers, a single dose of 43 mg was orally administered as a native or micellar formulation. The major human xanthohumol metabolites are quantified in plasma. Unmetabolized free xanthohumol makes 1% or less of total plasma xanthohumol. The area under the plasma concentration–time curve of xanthohumol-7-O-glucuronide following the ingestion of the micellular formulation is 5-fold higher and its maximum plasma concentration is more than 20-fold higher compared to native xanthohumol.

Conclusion: Metabolism of orally ingested xanthohumol is complex and efficiently converts the parent compound to predominantly glucuronic acid and to a lesser extent sulfate conjugates. The oral bioavailability of micellar xanthohumol is superior to native xanthohumol, making it a useful delivery form for future human trials.

1. Introduction

Many prenylated flavonoids native to hops have been studied for their health-beneficial and disease-preventive or even therapeutic activities.[1] The structurally related prenylated chalcone xanthohumol (XN) has promising activities against metabolic syndrome and cancer,[2] antibacterial and anti-viral activities, and may even have potential as a treatment against coronavirus infections, such as SARS-CoV-2.[2–4] XN is well tolerated in humans and does not alter clinical biomarkers, body weight, vital signs, or health-related quality of life.[5]

Prenylated flavonoids and chalcones are more lipophilic than their non-prenylated congeners and may thus more easily traverse cell membranes, which may facilitate their absorption.[6] Following oral ingestion, XN reaches the stomach, where the low pH facilitates its partial isomerization to isoxanthohumol (IXN).[7] XN is then absorbed in the small intestine and transported

L. Buckett, V. Spindler, M. Rychlik
Analytical Food Chemistry
Technical University of Munich
Maximus-von-Imhof Forum 2, 85354 Freising, Germany

N. Sus, J. Frank
Department of Food Biofunctionality (140b)
Institute of Nutritional Sciences
University of Hohenheim
Garbenstraße 28, 70599 Stuttgart, Germany
E-mail: jan.frank@nutres.de
C. Schoergenhofer
Department of Clinical Pharmacology
Medical University of Vienna
Währinger Gürtel 18–20, Vienna 1090, Austria
E-mail: christian.schoergenhofer@meduniwien.ac.at

to the liver where it may undergo metabolism by phase II enzymes, which catalyze conjugation reactions with water-soluble groups, such as glucuronic acid (GlcA) or sulfate. In healthy humans, the extent of phase II metabolism to generate O-glucuronides and O-sulfates of XN, administered as single doses of 60 or 180 mg, was nearly 100%.[8] The conjugated metabolites are secreted with the bile into the gut and the majority excreted in the feces, the remaining metabolites as well as the unmetabolized parent compound are excreted in the urine.[9] In addition, unabsorbed XN and biliary metabolites may undergo further biotransformation by the colonic microbiota, which can demethylate XN, resulting in 6-prenylnaringenin (6-PN) and 8-prenylnaringenin (8-PN) formation.[9]

The limited absorption of XN and its rapid metabolism are hurdles in the translation of the in vitro activities of XN to in vivo applications.[8] One other major issue, as described above, is that XN spontaneously cyclizes in the acidic environment of the stomach.[10] Consequently, the incorporation of XN into formulations that protect it from the acidic gastric conditions may aid in its absorption. Therefore, strategies to enhance XN solubility and to protect it from degradation, such as PEGylated graphene oxide nanosheet formulations of XN,[11] cyclodextrin formulations of the analogue xanthohumol-C,[12] and a micellar XN formulation,[13] have been developed in order to enhance its absorption and its biological activities. A protein-rich spent hops matrix enhanced XN absorption compared to a control spent hops preparation in humans.[14] A micellar formulation of XN inhibited Western-type diet-induced hepatic steatosis, inflammation, glucose intolerance, and body weight gain in mice and resulted in XN plasma concentration in the range of 100–330 nmol L^{-1}, whereas no XN was detectable after administration of native XN, which therefore was largely without effect in this mouse trial.[13] To the best of our knowledge, no study has investigated the absorption of XN from a micellular formulation compared to native XN in humans.

Most analytical methods used to quantify XN in human and animal trials employ enzymatic hydrolysis of the phase II conjugates and thus only quantify the sum parameter *total XN* (free + conjugated), which does not give a detailed overview of the diversity of compounds circulating in blood.[2] We recently published the synthesis of reference compounds for some XN metabolites, which now enables their identification and absolute quantification.[15]

Therefore, the aim of the present study was to identify the main metabolites formed after oral consumption of native and micellar XN and investigate their pharmacokinetics individually.

2. Results and Discussion

The present work aimed at identifying the main plasma metabolites of orally ingested XN in healthy humans and describing their individual pharmacokinetics rather than using the often-employed approach of quantifying total XN, which is the sum of parent compound plus conjugated phase II metabolites, after enzymatic hydrolysis. A further aim was to investigate if the metabolite profiles differed between native and micellar XN, because we hypothesized that the latter would be better bioavailable.

In a randomized, double-blind, crossover human trial, plasma samples were taken before and up to 24 h after ingestion of a sin-gle dose of 43 mg native or micellar XN and the plasma concentrations of the main metabolites were quantified to follow their pharmacokinetics. To the best of our knowledge, this is the first study reporting quantitative data on individual conjugated XN metabolites in humans and their pharmacokinetics following the intake of a micellular versus a native XN formulation. The employed data dependant acquisition (DDA) LC-MS/MS methodology combined with MS-Dial evaluation allowed targeted and untargeted approaches to simultaneously quantify and qualify pharmacokinetic data. The method here additionally allowed tentative confirmation of many metabolites and increased our understanding of XN metabolism.

2.1. Detected Metabolites of Xanthohumol

Metabolites were found initially by using the correlation function in MS-Dial when selecting reference compounds that were synthesized in previous work[15] by manually searching for glucuronic acid conjugates with an m/z of M+ GlcA (where M is the theoretical mass of XN/IXN or 8-PN/6-PN) and having the characteristic pharmacokinetic profile compared with XN-7-O-GlcA. Therefore, once all of the samples were uploaded, the MS1 spectra were compared for similarities in the abundance profile, but then, to confirm, the structures were tentatively annotated based on their MS2 spectra. An example of a confirmed annotation is given in **Figure 1** and shows the MS1 spectra over time to a very accurate MS1 of 0.008 Da. The MS2 spectra were taken from these time points and, using a mirror plot, were compared to a similar retention time (less than 5 s) of the reference compounds. Using the nominal mass of XN-7-O-GlcA 529.1715 (±0.008 Da) and 8-PN-7-O-GlcA 515.1524 (±0.010 Da), we identified four compounds at identification confidence level 1 (reference compound identified) and a further four at an identification confidence level 2 (MS2 and retention time), according to Schymanski et al.[16] **Table 1** shows all tentatively and identified compounds.

2.2. Recoveries and Precision

The recoveries of the metabolites were measured by spiking blank plasma with reference standards either before or after work-up. The areas of the reference standard peaks from MS-Dial were then compared between those before and after sample work-up. In general, recoveries from the metabolites were within 70–105%, but two analytes (colored red in **Table 2**), namely 6-PN-7-O-GlcA and 8-PN-7-O-sulfate, did not perform well. The low recoveries might be due to interfering peaks from the blood sample or due to the compound behaving differently than the other compounds during the extraction procedure. The method used was derived from van Breemen et al. where they did not calculate the recovery.[17] Because they were never calculated, the authors' recoveries during untargeted analysis might be similar to ours.

A pooled sample (quality control) was injected 12 times during each batch (4 times during each day over 3 days) and due to dilution (as blank samples were mixed in) not all analytes were resolvable. It was difficult to get MS2 spectra of many of the low-abundance compounds as they were below the DDA threshold.
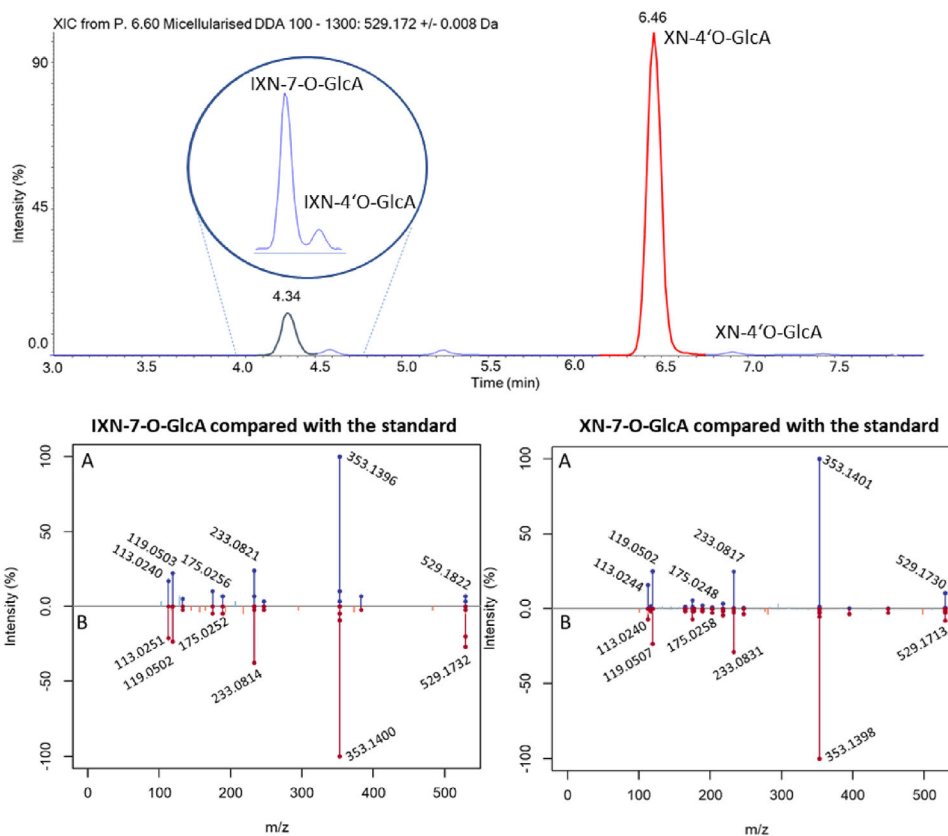
ADVANCED
SCIENCE NEWS

www.advancedsciencenews.com

Molecular Nutrition
Food Research

www.mnf-journal.com

Figure 1. Top: An LC-MS/MS chromatogram of the xanthohumol (XN) and isoxanthohumol (IXN) glucuronides. Below: A is the compound found in human plasma and B is the reference standard represented as MS2 mirror plots.

Hence only the higher-abundance compounds were calculated and are presented in **Table 3**. Within the results of the precision over 3 days, the method was below the 20% range across multiple metabolites. Data independent analysis (DIA) would complement future analysis of prenylated flavonoids as spectral libraries are produced in public databases. However, this information is limited, but from the results of this study they can be added for future analysis. Therefore, as more metabolites are known and found in databases, future analyses should apply DIA as recent results indicated the improved accuracy of quantification.[18]

2.3. Calibration Graphs

The concentrations of the metabolites with available reference standards were calculated by comparing the ratio of analyte reference standard with the closest eluting internal standard in regards to retention time. As all samples were co-injected with blank plasma, the calibration graphs were matrix-matched to minimize any matrix effects from the blood plasma ionization efficiencies. Calibration graphs were created for the following analytes: XN-7-O-GlcA, IXN-7-O-GlcA, 8-PN-7-O-GlcA, 6-PN-7-

Table 1. Identified metabolites and corresponding IDs.

Glucuronides	Sulfates	Mixed	Unknown	Free
XN-7-O-GlcA *	XN-7-O-sulfate	XN-sulfate-GlcA	(m/z) 425.1961	XN*
IXN-7-O-GlcA *	6-PN-7-O-sulfate*	8/6-PN-sulfate-GlcA	(m/z) 423.1827	IXN*
6-PN-7-O-GlcA*	8-PN-7-O-sulfate	XN-di-GlcA	(m/z) 531.1883	6-PN*
8-PN-7-O-GlcA*	XN-4'O-sulfate*	6/8-PN-di-GlcA	(m/z) 533.1957	8-PN*
XN-4'O-GlcA	IXN-4'O-sulfate	-	(m/z) 517.1365	-
IXN-4'O-GlcA	6-PN-4'-O-sulfate	-	-	-
8-PN-4'O-GlcA	8-PN-4'-O-sulfate	-	-	-
6-PN-4'O-GlcA	-	-	-	-

The (*) denotes that identification was based on reference standards. All other metabolites were identified by retention time, MS2 spectra, and pharmacokinetic profile matching similar to XN-7-O-GlcA (where applicable). See supplementary information for detailed annotation.

Table 2. The recoveries as % average and (RSD) of each metabolite where reference compounds where used.

	Glucuronide metabolites			
	XN-7-O-GlcA	6-PN-7-O-GlcA	8-PN-7-O-GlcA	IXN-7-O-GlcA
High	73 (7.4)	74 (4.6)	79 (11.5)	95 (2.6)
Medium	71 (8.8)	67 (2.5)	79 (11.5)	105 (2.3)
Low	76 (8.0)	63 (21)	92 (3.9)	93 (3.6)
	Sulfate metabolites			
	XN-4′-O-sulfate	6-PN-7-O-sulfate	8-PN-4′-O-sulfate	IXN-4′-O-sulfate
High	95 (5.6)	75 (2.8)	78 (12.4)	88 (6.5)
Medium	84 (11)	70 (0.8)	69 (18.1)	105 (2.3)
Low	86 (1.4)	87 (7.6)	89 (5.8)	82 (10.0)

O-GlcA, XN-4′-O-sulfate, IXN,4′-O-sulfate, 8-PN-4′-O-sulfate, 6-PN-7-O-sulfate, XN, and IXN. See Table S1, Supporting Information showing the corresponding internal standards and m/z of each compound.

2.4. Pharmacokinetics of Xanthohumol

The primary goal of the study identified and quantified the major metabolites of XN using reference standards.[15] As the blood plasma samples were not digested using glucuronidases and sulfatases, it was additionally possible to calculate the free XN (<1.2% of total XN) compared with the total XN amongst all participants ingesting the micellar formulation (**Figure 2**). Comparing the pharmacokinetic plot of XN-7-O-GlcA, scarcely any free XN was present in blood plasma (**Figure 3**). A study by Legette et al. revealed comparable values (<1%) with 60 or 180 mg XN orally ingested as a self-emulsifying mixture by humans, demonstrating that XN circulates to nearly 100% as conjugated metabolites.[8] Plasma AUC-$_{0–24\,h}$ were 19.7 nmol L^{-1} h^{-1} and C_{max} 10.6 nmol L^{-1} for unmetabolized micellar XN and 0.5 and 5 nmol L^{-1}, respectively, for native XN (Figure 2), indicating that the micellarised formulation is much better bioavailable and delivers higher amounts of free XN than native XN. T_{max} was not significantly different between formulations, although micellar XN reached peak concentrations in 0.8 h and native XN in 2.1 h, which is in agreement with the above study of Legette et al. using enzymatic deconjugation.[8]

The pharmacokinetic plots revealed two maxima at 30 and 480 min for conjugated XN, which suggests that it may be undergoing enterohepatic recirculation (Figure 3). The double maxima might be explained by biliary secretion of the conjugates into the intestine and hydrolysis of the conjugates by intestinal bacteria, thus releasing free XN back into the gut where re-absorption might occur. Free XN had a single maximum and the C_{max} of conjugated XN was ca. 100-fold higher than for free XN, suggest-

ing that conjugation of absorbed XN occurs rapidly and is nearly complete.

2.5. Pharmacokinetics of Xanthohumol Glucuronides

To the best of our knowledge, the present work is the first report of any XN glucuronides being quantified in humans. Glucuronides were the predominant XN conjugates, which is in agreement with previous findings,[5,8,14,19,20] although most of these studies did not quantify them as previously no reference standards were available.

The mean area under the plasma concentration–time curve (AUC) of **(1)** XN-7-O-GlcA was significantly higher following the consumption of micellar (250 nmol L^{-1} h^{-1}) than native XN (30 nmol L^{-1} h^{-1}), demonstrating the superior bioavailability of the micellar formulation (Figure 3). Also C_{max} was significantly higher (ca. 100-fold) after intake of micellar than native XN (Figure 3). These data are in agreement with previous findings in mice fed native or micellar XN for 3 weeks, in which total XN was not detectable following feeding of native XN, but plasma concentrations ranging from 100 to 330 nmol L^{-1} total XN were measured in mice fed the micellar formulation.[21] No differences were observed between micellar and native XN regarding T_{max} (Figure 3).

2.6. Pharmacokinetics of Xanthohumol Sulfates

The other major metabolite pathway for XN is sulfation resulting in metabolites XN-4′O-sulfate, 6-PN-7-O-sulfate, 8-PN-7-O-sulfate, and 6-PN-4′-O-sulfate (see supplementary information for semi-quantification results of 6-PN-4′-O-sulfate and MS2 spectra of the found sulfates). Reference standards were only available for XN-4′O-sulfate, which therefore was the only

Table 3. The precision of the method analyzing xanthohumol metabolites ($n = 12$) given as RSD percent of the mean over four times during the day and over 3 days.

XN-7-O-GlcA	IXN-7-O-GlcA	8-PN-7-O -GlcA	6-PN-7-O-GlcA	XN-4′O-sulfate	XN-sulfate-GlcA	(m/z) 531.1883	(m/z) 533.1957
6.4	3.3	10.4	14.8	13.7	16.6	5.4	10.5

ADVANCED
SCIENCE NEWS
www.advancedsciencenews.com
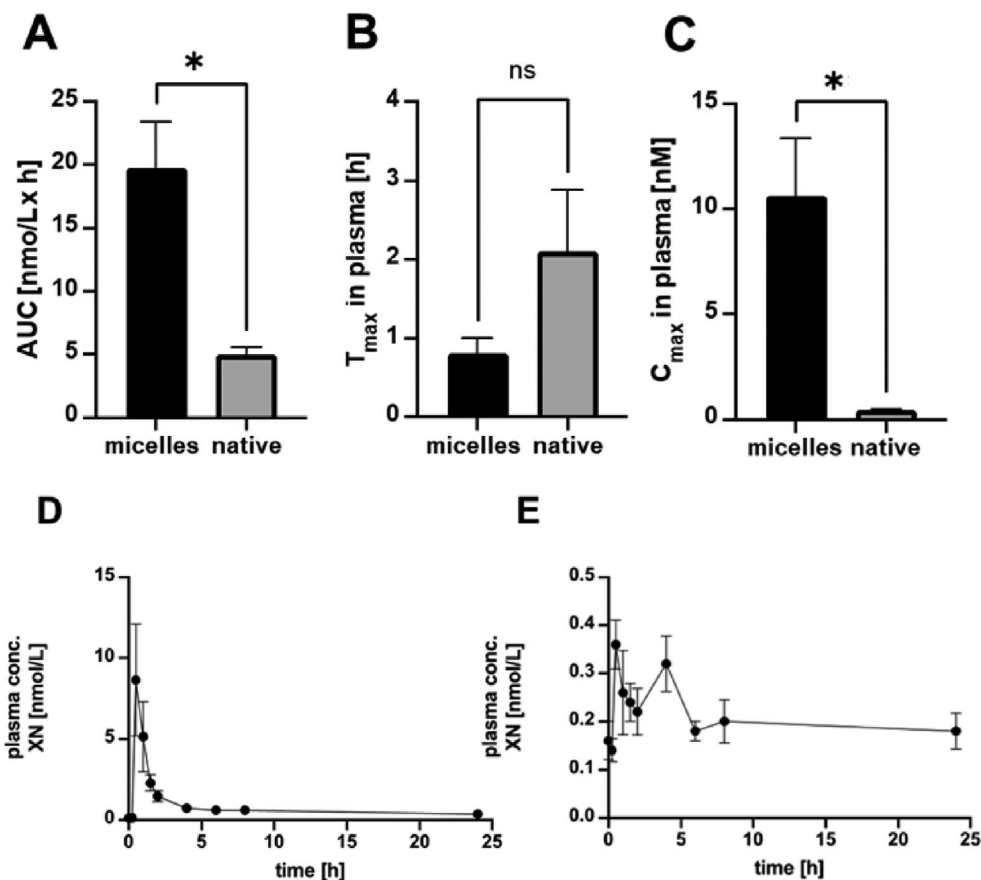
Molecular Nutrition
Food Research
www.mnf-journal.com

Figure 2. Mean ($n = 5$) xanthohumol (XN) area under the plasma concentration–time curve ($AUC_{0–24 h}$) (A), T_{max} (B), C_{max} (C), and plasma concentrations over time of XN following the ingestion of a single dose of 43 mg of micellar (D) or native XN (E); * significantly different at $p < 0.05$.

sulfate quantifiable in the micellular treatment, due to an interfering signal and no MS2 data in the native formulation. Furthermore, no peak was detected at the retention time for IXN-4′-O-sulfate at 5.1 min. There is, however, an equal peak at 5.5 min, which is actually in-source fragmentation (ISF) of XN-sulfate-GlcA, tentatively a xanthohumol-sulfate-glucuronic acid conjugate. Many sulfate and glucuronic acid metabolites of XN detected in our volunteers were also identified in postmenopausal women given a hop supplement.[17] However, we believe that in the latter study the annotation of xanthohumol-sulfate may have been incorrect and may also be in-source fragmentation of XN-sulfate-GlcA at the retention time of 5.7 min (**Figure 4**, see supplementary information for all annotation data).

Interestingly, the mean AUC (micellular) of the XN-4′-O-sulfate (280 nmol L^{-1} h^{-1}) was similar to that of XN-7-O-GlcA (251 nmol L^{-1} h^{-1}, **Figure 5**) despite the interfering signal at the same mass being present in all samples. The interference exaggerated the $AUC_{0–24 h}$ due to the zero point starting at 6 nmol L^{-1}. Therefore, the data are speculative but allow an estimation of the area under the curve revealing that the sulfates appear to peak at a similar time as the free XN glucuronic acid conjugates. In addition, as no MS2 information was found regarding the native XN supplementation, the micellular superiority in absorption is

demonstrated. Regarding the 8- and 6-prenylnaringenin sulfate conjugates, an ISF at 5.3 min was observed (see supplementary information), this could easily be mistaken as a 8-/6-PN-sulfate metabolite. 6-PN′-4′-O-sulfate and small amounts of the 6-PN-7-O-sulfate were also detected.

2.7. Identification and Pharmacokinetics of Mixed Xanthohumol Metabolites

As no reference compounds for mixed metabolites, containing both sulfates and glucuronides, were available, only tentative evidence for the annotation of these compounds was achieved. Two major mixed metabolites were XN-sulfate-GlcA and 6-/8-PN-sulfate-GlcA, which have the same order of magnitude (above 30,000 cps) as XN-7-O-GlcA. Because no reference compounds for these metabolites were available, we assumed that the concentrations are in a similar range and kept possible differences in ionization efficiencies in mind. Other found metabolites include double glucuronides (substances XN-di-GlcA and 6-/8-PN-di-GlcA). See the online supplementary material for all data regarding the annotations of mixed metabolites.

Two compounds that have similar pharmacokinetic profiles have revealed interesting features as their molecular masses (*m/z*
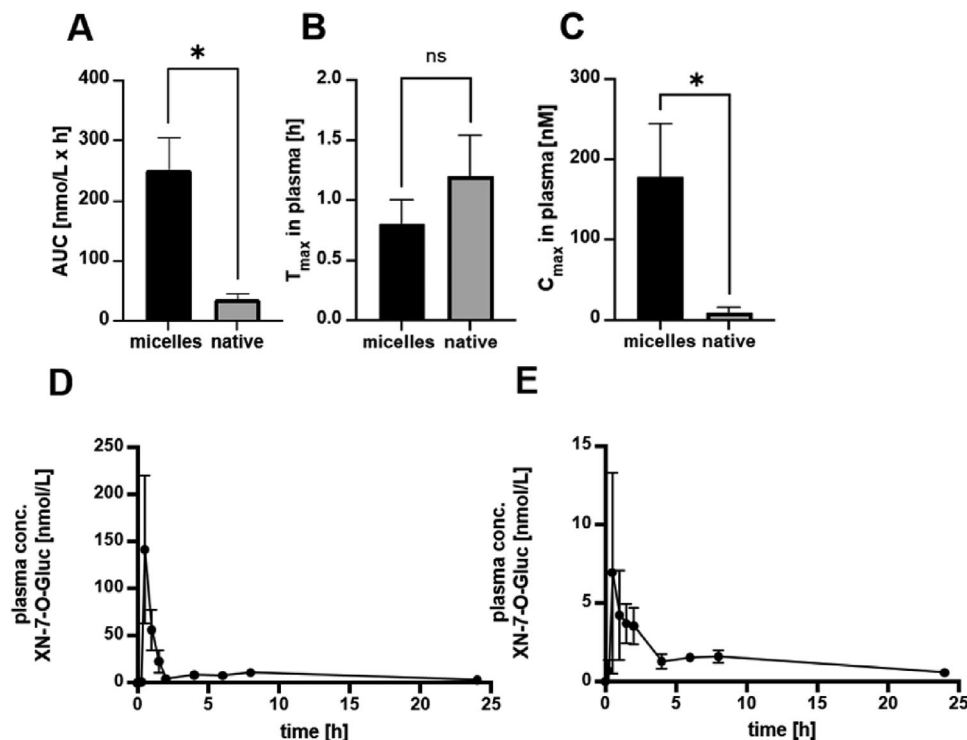
Figure 3. Mean ($n = 5$) XN-7-O-GlcA area under the plasma concentrations–time curve ($\text{AUC}_{0-24\,h}$) (A), T_{max} (B), C_{max} (C), and plasma concentrations over time of XN-7-O-GlcA following the ingestion of a single dose of 43 mg of micellar (D) or native XN; * significantly different at $p < 0.05$.

of 533.1672 and 531.1883) implying a hydrogenation reaction. To rule out that the compounds were present in the capsules, a sample was diluted 10,000-fold and analyzed using the same method (Figure S28, Supporting Information) and no parent masses of m/z of 355.1545 and 357.1352, which are theoretical deconjugated masses [M-GlcA]- containing the same MS2 spectra, were found.

Bacterial transformation of XN has been observed following in vitro digestion of IXN with *Eubacterium limosum*, which produces 8-PN.[22] Also *Eubacterium ramulus* is known to hydrogenate specifically the Michael system in many chalcones.[23]

While this may appear to suggest that bacteria were involved in the transformation of XN to 533.1672 and 531.1883, as it has the corresponding mass of M-2H in our volunteers, certain observations contradict this. Namely, the AUC for these metabolites were higher following the intake of micellar than native XN (**Figure 6**C), suggesting that they are derived from XN absorbed in the small intestine, as more unabsorbed native XN is expected the reach the colon. In addition the MS2 spectra are very different than reported by Miranda et al., therefore these compounds were not tentatively annotated.[24] This is further supported by the early appearance of these metabolites within 2 h after intake
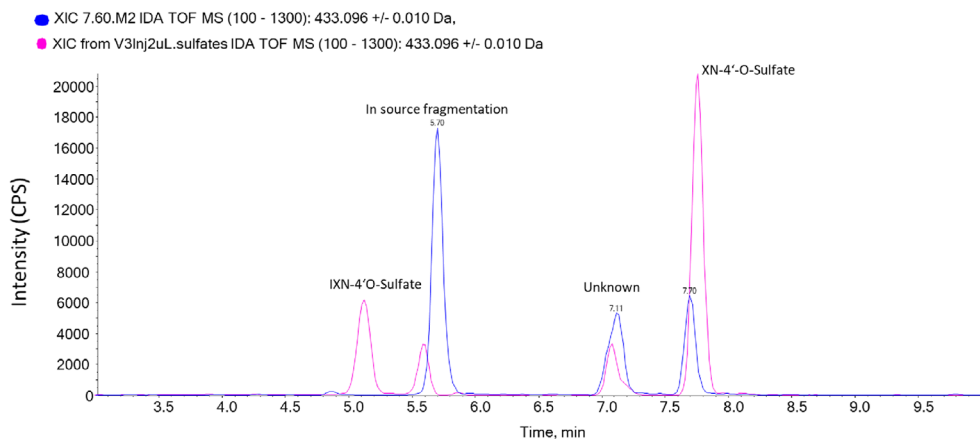

Figure 4. An extracted ion chromatogram of 433.0960 m/z analyzing the reference standards (pink) and the human plasma (blue). The in-source fragmentation is from the glucuronide sulfate conjugate of XN-sulfate-GlcA, which is based on having the same retention time.
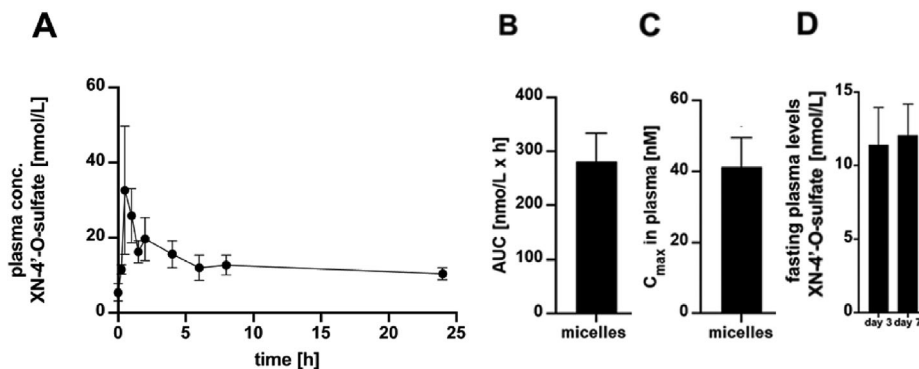
ADVANCED
SCIENCE NEWS
www.advancedsciencenews.com

Molecular Nutrition
Food Research
www.mnf-journal.com

Figure 5. Plasma concentrations over time of XN-4′-O-sulfate following the ingestion of a single dose of 43 mg of micellar (A). Mean ($n = 5$) XN-4′-O-sulfate area under the plasma concentrations–time curve ($AUC_{0–24 h}$) (B), and C_{max} (C) following the ingestion of a single dose of 43 mg of micellar. Fasting XN-4′-O-sulfate plasma concentrations after 3 and 7 days of daily ingestion of 129 mg micellar (D).

of XN, which is too short for compounds generated and absorbed in the colon. Hence, to answer the question where these metabolites originate from requires further experiments and cannot be answered with the presently available data. An additional compound that matched a demethylated version of m/z 531.1883 was also annotated as m/z 517.1365. Two additional compounds that followed similar pharmacokinetic data were not able to be annotated (m/z 425.1961) and (m/z 423.1827).

2.8. Pharmacokinetics of the Sum of Xanthohumol and its Metabolites

Combining all of the pharmacokinetic data from the quantified XN metabolites allowed us to show that significant absorption from the native and micellar formulations into the blood circulatory system occurred (**Figure 7**). The AUC of the sum of all XN and its metabolites quantified (apart from XN-4′O-sulfate due to

an interfering signal) was significantly higher after intake of 43 mg of micellar than native XN (Figure 7C). T_{max} was significantly shorter for micellar (1 h) than native (1.5 h) XN (Figure 7D). The terminal elimination half-life could not be calculated due to increasing concentrations between 5 and 24 h, although a long half-life of native XN has been observed previously.[20]

Even though significant differences in the bioavailability of single doses of micellar and native XN were observed in the present human trial, fasting blood concentrations of the sum of all XN metabolites did not significantly differ after 3 or 7 days of daily intake of 129 mg XN (one 43 mg capsule with each principle meal) (Figure 7F). However, a small increase in fasting total XN from day 3 to day 7 was observed when micellar XN was taken. In a similar trial comparing native versus micellar curcumin, significantly higher fasting curcumin concentrations were observed after intake of the micellar compared to the native formulation at days 3 and 7.[25] The differences may be explained by differences
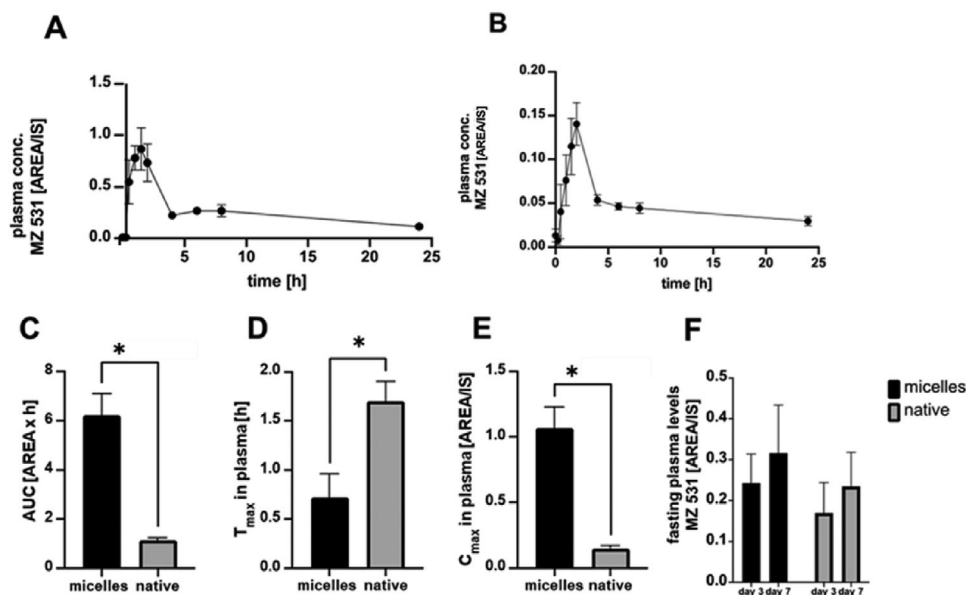

Figure 6. Plasma concentrations over time of m/z 531.1883 following the ingestion of a single dose of 43 mg of micellar (A) or native XN (B); mean ($n = 5$) 531.1883 area under the plasma concentrations–time curve ($AUC_{0–24 h}$) (C), T_{max} (D), C_{max} (E), fasting levels comparing the micellular and native dosage (F). * significantly different at $p < 0.05$.
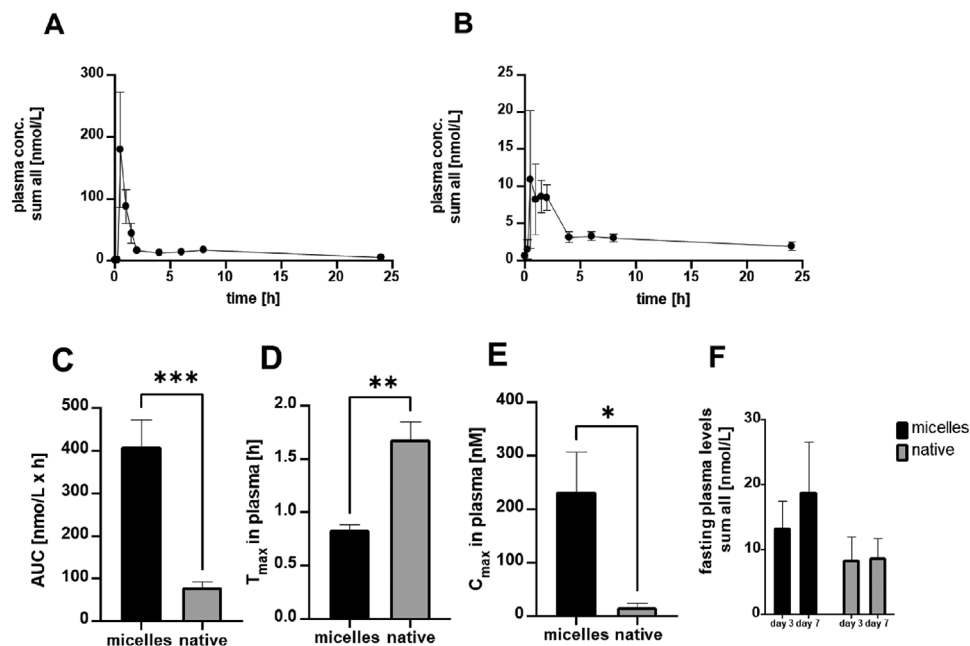
Figure 7. Plasma concentrations over time of all quantified metabolites following the ingestion of a single dose of 43 mg of micellar (A) or native xanthohumol (B); mean ($n = 5$) area under the plasma concentrations–time curve (AUC$_{0-24 h}$) (C), T_{max} (D), and C_{max} (E) of all metabolites. Fasting concentrations of the sum of all quantified metabolites after 3 and 7 days of daily ingestion of 129 mg micellar or native XN (F). * significantly different at $p < 0.05$.

in the solubilities of the compounds. The lipid-soluble curcumin is insoluble in water and dependent on conjugation with glucuronic acid and sulfates for its excretion, whereas XN is slightly soluble in water and can thus be more easily excreted.[26] The main metabolites found were glucuronides, sulfates, and mixed metabolites for both formulations. Compared to native XN, C_{max} for the main metabolites were more than 20-fold higher for micellar formulation. From the results we have compiled an updated metabolic pathway of XN (**Figure 8**).[9,17,23] XN is consumed and isomerized into IXN in the stomach followed by combinations of modifications (e.g., demethylation) creating a number of pre-metabolites for the liver to actively produce extensive glucuronidation and sulfation products. The bioactivities of the metabolites are yet to be investigated and are paramount in understanding the effects of XN consumption on health.

3. Conclusion

The present study, for the first time, quantified individual metabolites of xanthohumol (XN) following the ingestion of native or micellar formulations. XN-7-O-GlcA and XN-4′-O-sulfate were the quantitatively most important metabolites. Smaller quantities of mixed metabolites containing sulfates and glucuronides as well as double glucuronide conjugates of XN and derived prenylated chalcones and flavonoids were also found. Free XN made up only about 1% or less of total XN in our volunteers, suggesting efficient conjugation of XN by phase II enzymes. The plasma concentrations of free XN, XN-7-O-GlcA, and of the sum of all XN metabolites were significantly higher following the intake of micellar compared to native XN, demonstrating the supe-

rior bioavailability of the micellar formulation and suggesting it may be a useful delivery form for future human trials investigating biological activities of XN.

4. Experimental Section

Human Trial: This double-blind, randomized crossover trial was conducted at the Department of Clinical Pharmacology of the Medical University of Vienna between October 2018 and August 2019 with the approval of an independent ethics committee (ethics number 1580/2018). All participants gave their oral and written informed consent and were free to withdraw from the trial at any time. Five healthy volunteers (three males and two females) received in random order a single capsule containing 43 mg of native or micellar XN after an overnight fast. Blood samples were drawn before and 0.25, 0.5, 1, 1.5, 2, 4, 6, 8, and 24 h after ingestion of the capsule. After this initial pharmacokinetic phase, the volunteers received one capsule of XN (43 mg) with each principal meal (3 times per day) for 7 days. A final blood sample was drawn after 7 days of drug intake to investigate possible accumulation. A washout period of at least 7 days was maintained before crossover to the respective other treatment. Blood samples were centrifuged at 2000 × g for 15 min at 4 °C. Plasma was aliquoted and stored at −80 °C until analysis.

Blood Pre-Treatment: Plasma samples were analyzed in duplicate and 150 μL plasma was spiked with 0.25 mg L^{-1} internal standards (IXN-D3, 8-PN-D3, 6-PN-D3, and XN-D3; synthesized previously).[27] Extraction and clean-up were performed according to van Breemen et al.[17]

Calibration: Reference standards were dissolved in acetonitrile:methanol (90:10, by volume) at the following initial concentrations: XN-4′O-sulfate (0.114 mg L^{-1}), IXN-4′-O-sulfate (0.110 mg L^{-1}), 8-PN-4′-O-sulfate (0.109 mg L^{-1}), 6-PN-7-O-sulfate (0.106 mg L^{-1}), XN-7-O-glucuronide (0.263 mg L^{-1}), IXN-7-O- glucuronide (0.109 mg L^{-1}), 8-PN-7-O-glucuronide (0.195 mg L^{-1}), and 6-PN-7-O-glucuronide (0.144 mg L^{-1}). The free compounds XN, IXN, 8-PN, and 6-PN were dissolved

ADVANCED
SCIENCE NEWS
www.advancedsciencenews.com

Molecular Nutrition
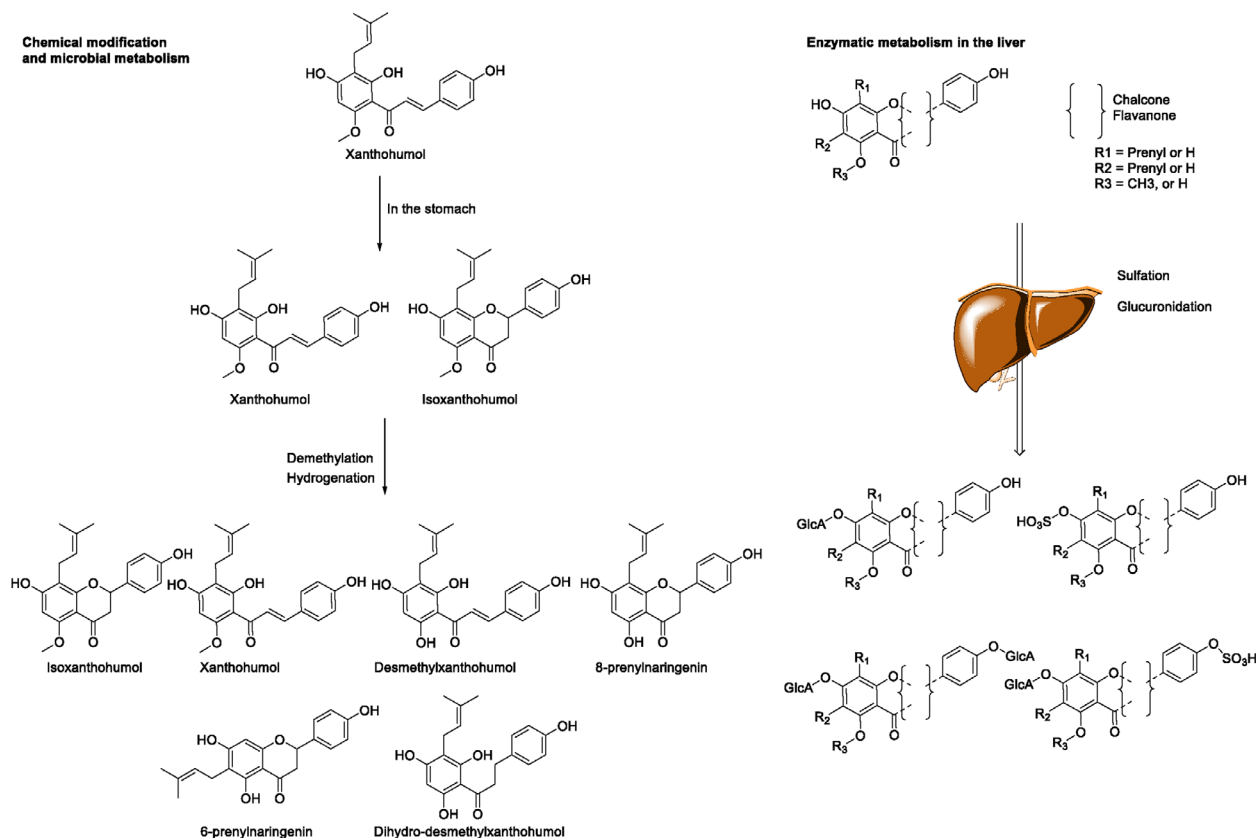Food Research
www.mnf-journal.com

Figure 8. Human metabolism of XN and related prenylated flavonoids in vivo. No hydroxylated compounds, mercapturic acid, and no direct glutathione adducts were detected in this study.

at a concentration of 0.01 mg L^{-1}. The highly concentrated substances were then diluted 10- and 100-fold, generating high, medium, and low concentration stock solutions for each substance. The stock solutions were co-injected using the autosampler at injection volumes ranging from 0.5 to 5.0 µL with a blank plasma sample containing the internal standards (0.25 mg L^{-1}) in a separate vial and injected into the LC-MS/MS using the same method. See Table S1, Supporting Information.

Recoveries: Blank blood plasma (free from prenylated flavonoids) was spiked with concentrations at three different concentrations (high: XN-7-O-GlcA [0.026 mg L^{-1}], IXN-7-O-GlcA [0.011 mg L^{-1}], 8-PN-7-O-GlcA [0.020 mg L^{-1}], 6-PN-7-O-GlcA [0.014 mg L^{-1}], XN-4′-O-sulfate [0.011 mg L^{-1}], 6-PN-7-O-sulfate [0.011 mg L^{-1}] and 8-PN-4′-O-sulfate [0.011 mg L^{-1}]). The medium recoveries were tested at half the concentration as the high values and low recovery were tested at a 10-fold dilution of the high values. The recoveries were then calculated of the theoretical (spiked concentration) versus the calculated result using the determined calibration graphs. The lower limit of detection (LOD) was set at a peak found over 500 cps in height and the lower limit of quantification (LOQ) was estimated between the lowest and second lowest calibration points.

LC-MS/MS: LC-MS/MS was carried out on a Sciex Exion LC AD system coupled to a Sciex X500R QToF-MS (MDS Sciex, Concord, Canada). The system was calibrated every five samples and operated in information dependant acquisition (IDA) mode (also known as DDA). The ms range was set between 100 and 800 *m/z* and a selection of 10 precursors was set with a collision energy at 35 eV with a spread of 15 eV and fragmentation events above counts of 1000. The analytes were separated using the LC method developed by Buckett et al. (Supplementary information).[15] Each participant's samples were randomized and data were collected on a batch to batch within a time of 3 weeks.

MS-Dial and MS Convert: The Wiff. files were converted to mzML files using the Windows version of MS_convert and then grouped into the micellar and native groups manually.[28] Each participant's sample files were then incorporated into MS-dial (version 4.8 http://prime.psc.riken.jp/compms/msdial/main.html) using the following parameters, Ms1 and Ms2 tolerance of 0.05 Da, Ms range 338–1000 Da and MS/MS 100–1300 Da. Peak detection of 1000 amplitude and a mass slice of 0.5 Da with a smoothing level of 3 and a minimum peak of 10 scans. The MS/MS cut-off was set at 5. Due to computational limitations, each participant was uploaded individually and the alignment file used was 60 min. All known compounds were annotated manually and the metabolites' integrations at each time point were copied into Microsoft Excel (Excel 2019, Microsoft, WA, USA). The metabolites were found by comparing known reference standards features (MS, MS2, retention time pharmacokinetic profile) and the correlation feature in MS-dial (similar to Pearson correlation). The same process was applied to the calibration samples and graphs were produced using Microsoft Excel.

XCMS and See MS: To visualize some non-target MS2 spectra, the programme SeeMS (64-bit, version 3.0.21173.0) was used to extract MS2 spectra on a Windows 11 machine (SQ1 processor with 16 Gb RAM). These MS2 spectra were again processed using the XCMS programme in R-studio (version R 4.1.3).[29]

Statistical Analysis: Using the integrals of each peak obtained from MS-Dial calibration graphs were constructed. The linear trend line function was used and the concentrations of each analyte were calculated using linear regression extrapolation in Microsoft Excel. Using the concentrations that were calculated from Excel, pharmacokinetic plots were produced by plotting the concentration or compound ratio (qualitative analysis) over the retention time. All statistical analyses, including the calculation of AUC, were conducted with GraphPad Prism 9 (version 9.0.0, GraphPad Software, San Diego, CA, USA). Results were presented as arithmetic

mean with standard deviation (SD) or with standard error of the mean (SEM). Differences between the formulations regarding AUC, C_{max}, and t_{max} were computed by repeated-measures ANOVA followed by a Tukey post hoc test. Differences were considered significant at $p < 0.05$.

Supporting Information

Supporting Information is available from the Wiley Online Library or from the author.

Conflict of Interest

J.F. is a scientific consultant to AQUANOVA AG, the company producing micellular formulations of xanthohumol.

Author Contributions

L.B., C.S., J.F., and M.R. conceptualized the project. C.S. carried out the human trial. L.B. and V.S. carried out the sample work-up of the samples. L.B. carried out the analysis of the samples. L.B. and N.S. carried out the data analysis. L.B. and M.R. wrote the initial draft, which was revised by L.B., M.R., C.S., and J.F. All authors agreed to the manuscript before submission.

Data Availability Statement

The data that support the findings of this study are available from the corresponding author upon reasonable request.

[1] S. Venturelli, M. Burkard, M. Biendl, U. Lauer, J. Frank, C. Busch, *Nutrition* **2016**, *32*, 1171.
[2] H. F. Neumann, J. Frank, S. Venturelli, S. Egert, *Mol. Nutr. Food Res.* **2022**, *66*, 2100831.
[3] Y. Lin, R. Zang, Y. Ma, Z. Wang, L. Li, S. Ding, R. Zhang, Z. Wei, J. Yang, X. Wang, *Int. J. Mol. Sci.* **2021**, *22*, 12134.
[4] S. Yuan, B. Yan, J. Cao, Z.-W. Ye, R. Liang, K. Tang, C. Luo, J. Cai, H. Chu, T. W.-H. Chung, K. K.-W. To, I. F.-N. Hung, D.-Y. Jin, J. F.-W. Chan, K.-Y. Yuen, *Cell Discov.* **2021**, *7*, 100.
[5] B. O. Langley, J. J. Ryan, D. Hanes, J. Phipps, E. Stack, T. O. Metz, J. F. Stevens, R. Bradley, *Mol. Nutr. Food Res.* **2021**, *65*, 2001170.
[6] X. Chen, E. Mukwaya, M.-S. Wong, Y. Zhang, *Pharm. Biol.* **2014**, *52*, 655.
[7] D. Nikolic, Y. Li, L. R. Chadwick, G. F. Pauli, R. B. van Breemen, *J. Mass Spectrom.* **2005**, *40*, 289.
[8] L. Legette, C. Karnpracha, R. L. Reed, J. Choi, G. Bobe, J. M. Christensen, R. Rodriguez-Proteau, J. Q. Purnell, J. F. Stevens, *Mol. Nutr. Food Res.* **2014**, *58*, 248.
[9] L. Hanske, G. Loh, S. Sczesny, M. Blaut, A. Braune, *Mol. Nutr. Food Res.* **2010**, *54*, 1405.
[10] S. Possemiers, A. Heyerick, V. Robbens, D. De Keukeleire, W. Verstraete, *J. Agric. Food Chem.* **2005**, *53*, 6281.
[11] J. Zhang, L. Yan, P. Wei, R. Zhou, C. Hua, M. Xiao, Y. Tu, Z. Gu, T. Wei, *Eur. J. Pharmacol.* **2021**, *895*, 173866.
[12] M. Kirchinger, L. Bieler, J. Tevini, M. Vogl, E. Haschke-Becher, T. K. Felder, S. Couillard-Després, H. Riepl, C. Urmann, *Planta Med.* **2019**, *85*, 1233.
[13] A. Mahli, T. Seitz, K. Freese, J. Frank, R. Weiskirchen, M. Abdel-Tawab, D. Behnam, C. Hellerbrand, *Cells* **2019**, *8*, 359.
[14] A. O'Connor, V. R. Konda, R. L. Reed, J. M. Christensen, J. F. Stevens, N. Contractor, *Mol. Nutr. Food Res.* **2018**, *62*.
[15] L. Buckett, S. Schönberger, V. Spindler, N. Sus, C. Schoergenhofer, J. Frank, O. Frank, M. Rychlik, *Metabolites* **2022**, *12*, 345.
[16] E. L. Schymanski, J. Jeon, R. Gulde, K. Fenner, M. Ruff, H. P. Singer, J. Hollender, *Environ. Sci. Technol.* **2014**, *48*, 2097.
[17] R. B. van Breemen, L. Chen, A. Tonsing-Carter, S. Banuvar, E. Barengolts, M. Viana, S.-N. Chen, G. F. Pauli, J. L. Bolton, *J. Agric. Food Chem.* **2020**, *68*, 5212.
[18] C. Fernández-Costa, S. Martínez-Bartolomé, D. B. McClatchy, A. J. Saviola, N.-K. Yu, J. R. Yates, *J. Proteome Res.* **2020**, *19*, 3153.
[19] S. Bolca, J. Li, D. Nikolic, N. Roche, P. Blondeel, S. Possemiers, D. De Keukeleire, M. Bracke, A. Heyerick, R. B. van Breemen, H. Depypere, *Mol. Nutr. Food Res.* **2010**, *54*, S284.
[20] R. B. van Breemen, Y. Yuan, S. Banuvar, L. P. Shulman, X. Qiu, R. F. R. Alvarenga, S.-N. Chen, B. M. Dietz, J. L. Bolton, G. F. Pauli, E. Krause, M. Viana, D. Nikolic, *Mol. Nutr. Food Res.* **2014**, *58*, 1962.
[21] A. Mahli, T. Seitz, K. Freese, J. Frank, R. Weiskirchen, M. Abdel-Tawab, D. Behnam, C. Hellerbrand, *Cells* **2019**, *8*, 359.
[22] E. Moens, S. Bolca, T. Van de Wiele, A. Van Landschoot, J. L. Goeman, S. Possemiers, W. Verstraete, *AMB Express* **2020**, *10*, 79.
[23] I. L. Paraiso, L. S. Plagmann, L. Yang, R. Zielke, A. F. Gombart, C. S. Maier, A. E. Sikora, P. R. Blakemore, J. F. Stevens, *Mol. Nutr. Food Res.* **2019**, *63*, 1800923.
[24] C. L. Miranda, L. A. Johnson, O. de Montgolfier, V. D. Elias, L. S. Ullrich, J. J. Hay, I. L. Paraiso, J. Choi, R. L. Reed, J. S. Revel, C. Kioussi, G. Bobe, U. T. Iwaniec, R. T. Turner, B. S. Katzenellenbogen, J. A. Katzenellenbogen, P. R. Blakemore, A. F. Gombart, C. S. Maier, J. Raber, J. F. Stevens, *Sci. Rep.* **2018**, *8*, 613.
[25] J. Grafeneder, U. Derhaschnig, F. Eskandary, N. Buchtele, N. Sus, J. Frank, B. Jilma, C. Schoergenhofer, *Mol. Nutr. Food Res.* **2022**, *66*, e2200139.
[26] D. Kostrzewa, A. Dobrzyńska-Inger, E. Rój, *Fluid Phase Equilib.* **2013**, *360*, 445.
[27] L. Buckett, S. Schinko, C. Urmann, H. Riepl, M. Rychlik, *Front. Nutr.* **2020**, *7*, 619921.
[28] M. C. Chambers, B. Maclean, R. Burke, D. Amodei, D. L. Ruderman, S. Neumann, L. Gatto, B. Fischer, B. Pratt, J. Egertson, K. Hoff, D. Kessner, N. Tasman, N. Shulman, B. Frewen, T. A. Baker, M.-Y. Brusniak, C. Paulse, D. Creasy, L. Flashner, K. Kani, C. Moulding, S. L. Seymour, L. M. Nuwaysir, B. Lefebvre, F. Kuhlmann, J. Roark, P. Rainer, S. Detlev, T. Hemenway, et al., *Nat. Biotechnol.* **2012**, *30*, 918.
[29] J. Rainer, A. Vicini, L. Salzer, J. Stanstrup, J. M. Badia, S. Neumann, M. A. Stravs, V. Verri Hernandes, L. Gatto, S. Gibb, M. Witting, *Metabolites* **2022**, *12*.